Protein phosphatase 2Cm is a critical regulator of branched-chain amino acid catabolism in mice and cultured cells

Gang Lu,[1] Haipeng Sun,[1] Pengxiang She,[2] Ji-Youn Youn,[1] Sarah Warburton,[1] Peipei Ping,[3] Thomas M. Vondriska,[1,3] Hua Cai,[1] Christopher J. Lynch,[2] and Yibin Wang[1,3,4]

[1]Division of Molecular Medicine, Department of Anesthesiology, David Geffen School of Medicine, UCLA, Los Angeles, California, USA.
[2]Department of Cellular and Molecular Physiology, Penn State College of Medicine, Hershey, Pennsylvania, USA.
[3]Departments of Physiology and Medicine, David Geffen School of Medicine, and [4]Molecular Biology Institute, UCLA, Los Angeles, California, USA.

The branched-chain amino acids (BCAA) are essential amino acids required for protein homeostasis, energy balance, and nutrient signaling. In individuals with deficiencies in BCAA, these amino acids can be preserved through inhibition of the branched-chain-α-ketoacid dehydrogenase (BCKD) complex, the rate-limiting step in their metabolism. BCKD is inhibited by phosphorylation of its E1α subunit at Ser293, which is catalyzed by BCKD kinase. During BCAA excess, phosphorylated Ser293 (pSer293) becomes dephosphorylated through the concerted inhibition of BCKD kinase and the activity of an unknown intramitochondrial phosphatase. Using unbiased, proteomic approaches, we have found that a mitochondrial-targeted phosphatase, PP2Cm, specifically binds the BCKD complex and induces dephosphorylation of Ser293 in the presence of BCKD substrates. Loss of PP2Cm completely abolished substrate-induced E1α dephosphorylation both in vitro and in vivo. PP2Cm-deficient mice exhibited BCAA catabolic defects and a metabolic phenotype similar to the intermittent or intermediate types of human maple syrup urine disease (MSUD), a hereditary disorder caused by defects in BCKD activity. These results indicate that PP2Cm is the endogenous BCKD phosphatase required for nutrient-mediated regulation of BCKD activity and suggest that defects in PP2Cm may be responsible for a subset of human MSUD.

Introduction

The branched-chain amino acids (BCAA), including leucine, isoleucine, and valine, are essential amino acids that participate in the de novo synthesis and structural maintenance of nascent protein and biosynthesis of alanine and glutamine for energy balance and anaplerosis. They also provide a nutrient signal that heralds the presence of protein-containing meals. BCAA regulate protein translation, protein turnover, and cellular growth and may additionally modulate appetite (1, 2). Supplementation of BCAA has been associated with improved body weight control and glycemia (3–5). On the other hand, deficiencies of BCAA impair normal growth and development (6). A complete or partial block in the second step of BCAA metabolism catalyzed by branched-chain-α-ketoacid dehydrogenase (BCKD) leads to the accumulation of BCAA and their potentially cytotoxic α-ketoacid derivatives (branched-chain-α-ketoacids [BCKA]). The cytotoxicity of the BCKA is evident in maple syrup urine disease (MSUD), a genetic disorder characterized by devastating clinical symptoms, including fatal ketoacidosis, coma, convulsions, mitochondrial dysfunction, psychomotor delay, and mental retardation (7–9).

The first step in BCAA catabolism is catalyzed by either a cytosolic or mitochondrial isoform of branched-chain aminotransferase (10–12). Through this rapid, high capacity, and reversible reaction, leucine, isoleucine, and valine are converted into α-ketoisocaproate (KIC), α-keto-β-methylvalerate, and α-ketoisovalerate, respectively (1, 13). The next is the first committed and rate-limiting step in the metabolic pathway, which is catalyzed by BCKD. This highly regulated, multienzyme protein complex contains several enzymatic activities that share similar genomic, structural, and biochemical features with the pyruvate dehydrogenase and α-ketoglutarate dehydrogenase (14, 15). Mammalian BCKD complex contains 24 copies of dihydrolipoyl transacylase (E2 component), multiple copies of the branched-chain-α-ketoacid-decarboxylase (E1 component), each containing 2 E1α and E1β subunits, and a dihydrolipoamide dehydrogenase (E3 component) (15–17). To date, more than 100 mutations in genes encoding E1α, E1β, E2, and E3 subunits have been identified in humans, leading to a broad spectrum of MSUD symptoms (13). However, the molecular basis of many of the less severe but nevertheless potentially lethal and debilitating forms, such as intermediate and intermittent MSUD, remains to be determined.

As a rate-limiting enzyme in BCAA catabolism, BCKD activity is tightly regulated under different growth and nutrient environments to ensure a steady plasma level of BCAA. Previous studies have shown that one of the major mechanisms in BCKD regulation is the reversible phosphorylation of the E1α subunit at Ser293 residue (13, 17–20). Under low levels of BCAA, BCKD is inactivated through phosphorylation at Ser293 of its E1α subunit. In the presence of BCAA and BCKA, BCKD becomes activated as Ser293 is dephosphorylated, presumably through an intramitochondrial phosphatase (18, 21, 22). Despite the longstanding recognition of its importance, the search in the past

Conflict of interest: The authors have declared that no conflict of interest exists.

Nonstandard abbreviations used: BCAA, branched-chain amino acids; BCKA, branched-chain-α-ketoacids; BCKD, branched-chain-α-ketoacid dehydrogenase; KIC, α-ketoisocaproate; MEF, mouse embryonic fibroblast; MSUD, maple syrup urine disease; pSer293, phosphorylated Ser293.

Citation for this article: *J. Clin. Invest.* **119**:1678–1687 (2009). doi:10.1172/JCI38151.

2 decades for the molecular identity of the endogenous BCKD phosphatase has been unsuccessful, leaving much of the underlying mechanisms in BCAA catabolic regulation unexplored.

Recently, we discovered a novel mitochondrial matrix resident type 2C phosphatase gene, *PP2Cm* (also named *PPM1K*), and demonstrated that it is essential for cell survival and normal development (23). Its expression is downregulated in the heart under stress conditions (23). Loss of *PP2Cm* rendered cells sensitive to calcium-induced mitochondrial permeability transition and promoted apoptotic cell death in isolated neonatal cardiomyocytes, mouse liver, and developing zebrafish embryos. However, the underlying molecular mechanism in PP2Cm-mediated mitochondrial and cellular regulation was not clear. Shortly after that, Joshi et al. (14) reported that recombinant PP2Cm can dephosphorylate BCKD purified from rat liver. While this suggested the potential for PP2CM to play a role in BCAA catabolism, other phosphatases also possess this activity in vitro. In this report, we employed unbiased biochemical and discovery proteomic approaches that led to the identification of BCKD E1α, E1β, and E2 subunits as PP2Cm-interacting partners in mitochondria. Ectopic expression of PP2Cm was sufficient to dephosphorylate E1α phosphorylated Ser293 (pSer293) in cultured cells. On the other hand, loss of PP2Cm completely abolished E1α dephosphorylation induced by BCKA substrates in *PP2Cm*$^{-/-}$ mouse embryonic fibroblasts (MEFs) or *PP2Cm*$^{-/-}$ animals. These findings led us to conclude that PP2Cm is the endogenous BCKD phosphatase critical to nutrient-induced activation of BCKD. *PP2Cm*$^{-/-}$ animals exhibited similar metabolic phenotype as MSUD patients, and *PP2Cm*$^{-/-}$ neonates had substantially higher incidence of mortality when maintained on a high-protein diet. At least 5 human SNPs in the *PP2Cm* coding sequence have already been listed in GenBank, prompting us to speculate that PP2Cm deficiency or mutations leading to PP2Cm dysfunction may represent what we believe to be a novel etiology and a therapeutic target for those with intermediate and/or intermittent types of MSUD.

Results

Identification of phosphorylated BCKD complex as a PP2Cm substrate in cells. PP2Cm is a newly characterized member of the PP2C Ser/Thr phosphatase family. It is located exclusively in mitochondrial matrix and has a critical role in cell survival and vertebrate development (23). To uncover the underlying molecular mechanisms of these phenotypic effects, we sought to identify the potential substrate(s) of PP2Cm through a biochemical purification approach. We established stable HEK293 (Figure 1) and INS-1 (Supplemental Figure 1; supplemental material available online with this article; doi:10.1172/JCI38151DS1) cell lines expressing PP2Cm protein tagged with both FLAG and HA at its carboxyl terminus. Through sequential purification with anti-FLAG and anti-HA columns, PP2Cm protein complex was purified to near homogeneity. Three specific co-purified protein species were identified on silver-stained SDS PAGE gels (Figure 1A), and their molecular identities were analyzed by using liquid chromatography/tandem mass spectrometry (LC/MS/MS). The 3 specific binding proteins were identified as BCKD E2 subunit, E1α subunit, and E1β subunit, respectively (Supplemental Figure 1). The validity of the mass spectrometry results was confirmed by immunoblotting of the PP2Cm immunocomplex, using corresponding antibodies for E2, E1α, or total BCKD complex, respectively (Figure 1B). Notably, E3 subunit is absent from the PP2Cm immunocomplex.

To investigate the potential role for PP2Cm as an pSer293 E1α phosphatase in cells, we examined ectopically expressed PP2Cm in WT MEFs. Ectopic expression of PP2Cm induced substantial pSer293 dephosphorylation under both basal conditions and after incubation with 5 mM BCKA mixture (Figure 1C). Taken together, these results indicate that PP2Cm interacts with BCKD complex and is capable of dephosphorylating pSer293 E1α as a potential substrate.

Generation of PP2Cm-deficient mouse model. To further evaluate whether PP2Cm functions as the endogenous BCKD phosphatase, we generated *PP2Cm*-deficient mice via homologous recombination in ES cells. A LacZ-expressing cassette was inserted into the translational initiation site of the *PP2Cm* allele, while replacing the major portion of exon 2 of the mouse *PP2Cm* gene (Figure 2A). The engineered *PP2Cm* null allele in recombinant ES cells and the subsequently derived heterozygous and homozygous animals were confirmed by genomic DNA Southern blot analysis (Supplemental Figure 2). In *PP2Cm*$^{-/-}$ animals, LacZ staining demonstrated high-level expression in brain, heart, liver, and diaphragm, recapitulating the expression profile of the endogenous *PP2Cm* mRNA as previously reported (23) (Supplemental Figure 3). Complete loss of *PP2Cm* expression in the *PP2Cm*$^{-/-}$ heart was confirmed by quantitative RT-PCR (Figure 2B) and immunoblotting (Figure 2C). In contrast, *Bckdk* mRNA was not changed in the *PP2Cm*$^{-/-}$ heart (Figure 2B). The distribution of WT, *PP2Cm*$^{+/-}$, and *PP2Cm*$^{-/-}$ genotypes from *PP2Cm*$^{+/-}$ breeding pairs followed an expected Mendelian ratio (Supplemental Table 1). The *PP2Cm*$^{-/-}$ animals in a 129Sv/C57BL/6 background were generally viable and fertile when fed with a regular 18% protein diet and displayed no overt developmental abnormalities up to 1 year of age.

PP2Cm is the essential BCKD phosphatase in MEFs. To investigate whether *PP2Cm* deficiency has any impact on E1α phosphorylation, we used MEFs prepared from both *PP2Cm*$^{-/-}$ and WT embryos. Equivalent Ser293 E1α phosphorylation was detected in *PP2Cm*$^{-/-}$ and WT MEFs in either the basal conditions or after 2 hours of amino acid starvation (Figure 3A). Thirty minutes after treatment of BCKA, Ser293 E1α was completely dephosphorylated in WT MEFs but not in *PP2Cm*$^{-/-}$ cells (Figure 3A). This result suggests that PP2Cm is an essential phosphatase for pSer293 E1α dephosphorylation in cells. Figure 3A also shows that compared with incubation in DMEM cell culture media, the protein level of BCKD kinase was substantially increased after amino acid starvation and subsequently decreased following exposure to BCKA in both *PP2Cm*$^{-/-}$ and WT MEFs. However, the relative concentration of BCKD kinase protein was substantially lower in *PP2Cm*$^{-/-}$ MEFs compared with WT controls (Figure 3A). In contrast, *Bckdk* mRNA was not changed in *PP2Cm*$^{-/-}$ MEFs (Figure 2B).

We next attempted to determine whether the defect in pSer293 E1α dephosphorylation in *PP2Cm*$^{-/-}$ MEFs (Figure 3A) was specifically caused by the loss of PP2Cm. Using adenovirus-mediated gene transfer, we reintroduced either the WT or R236G, a phosphatase-dead mutant of PP2Cm, into *PP2Cm*$^{-/-}$ MEFs. As shown in Figure 3B, BCKA-stimulated dephosphorylation of pSer293 was restored by the WT PP2Cm but not the phosphatase-dead mutant. Moreover, in WT MEFs, ectopic expression of the WT PP2Cm enhanced pSer293 E1α dephosphorylation, while the phosphatase-dead mutant attenuated it, therefore functioning in a dominant-negative manner (Figure 3B). These data support the hypothesis that functional PP2Cm is fully responsible for E1α dephosphorylation activity.

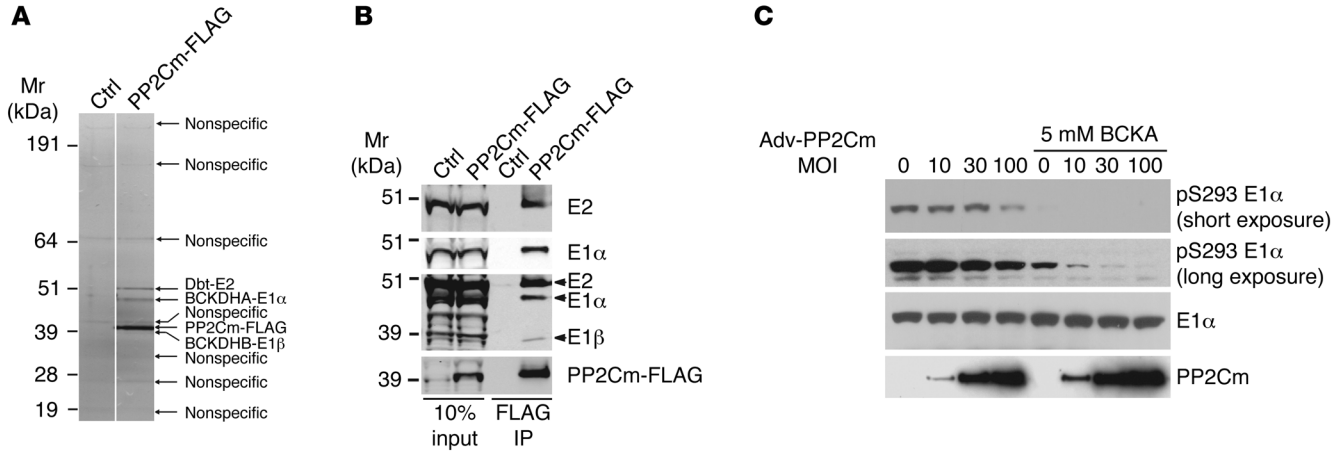

Figure 1

PP2Cm interacts with the BCKD complex and dephosphorylates E1α at Ser293. (**A**) The PP2Cm immunocomplex was isolated using anti-FLAG antibody from a HEK293T cell line stably expressing PP2Cm-FLAG and separated on SDS-PAGE. Based on mass spectrometry, the molecular identity of specific protein species, as shown in a silver staining gel, was revealed as labeled. Lanes were run on the same gel but were nonadjacent. BCKDHA-E1α, branched-chain ketoacid dehydrogenase E1, α polypeptide; BCKDHB-E1β, branched-chain ketoacid dehydrogenase E1, β polypeptide; Dbt-E2, dihydrolipoamide branched-chain transacylase E2; Mr, molecular weight; CTRL, control sample from parental HEK293T cells without PP2Cm-FLAG expression following the same immunoprecipitation procedure. (**B**) Immunoblotting on the same SDS-PAGE gel, using specific antibodies for E2, E1α, and anti-(E1+E2) antibodies, which recognize E2, E1α, and E1β subunits to differing extents. (**C**) Immunoblotting on the same SDS-PAGE gel for pSer293 (pS293) E1α, total E1α, and PP2Cm is shown on separate rows as indicated (25). MEFs infected with adenoviral vector expressing PP2Cm (Adv-PP2Cm), at different MOI as indicated, were left untreated or treated with 5 mM BCKA mixture.

To further test the specificity and relative contribution of PP2Cm in its BCKD phosphatase activity, WT or *PP2Cm*$^{-/-}$ MEFs were exposed to 5 mM BCKA for up to 8 hours; and the Ser293 E1α phosphorylation status was subsequently monitored. In WT MEFs, pSer293 E1α underwent robust dephosphorylation within 20 minutes of BCKA addition. However, it was only partially phosphorylated 3 hours later, presumably reflecting a gradual clearance of BCKA in the culture medium, leading to subsequent rephosphorylation of Ser293 (Figure 3C, upper panel). In *PP2Cm*$^{-/-}$ MEFs, however, the Ser293 E1α phosphorylation state was maintained for the entire 8 hours of BCKA exposure (Figure 3C, lower panel). These findings suggest that PP2Cm is indispensable and, most likely, the only mitochondrial BCKD phosphatase responsible for pSer293 dephosphorylation.

PP2Cm is required for E1α dephosphorylation in vivo. The above results demonstrate that PP2Cm is the essential BCKD phosphatase responsible for BCKA-stimulated Ser293 dephosphorylation in cultured cells. To determine whether PP2Cm plays a similar role in vivo, we evaluated Ser293 phosphorylation in various mouse tissues, including liver and heart from *PP2Cm*$^{-/-}$ animals (Figure 4A). It is well established that BCAA transamination occurs in extrahepatic organs, such as the heart, whereas BCKD-mediated oxidative decarboxylation is mostly active in the liver (2, 24). In WT mice with constant access to a standard 18% protein diet, hepatic Ser293 is hypophosphorylated (with some variation, perhaps due to random food intake), whereas cardiac Ser293 was hyperphosphorylated, consistent with a more activated state of the BCKD complex in liver relative to heart (Figure 4A). In contrast, hepatic pSer293 E1α was elevated in *PP2Cm*$^{-/-}$ mice fed with the same diet (Figure 4A). We have previously shown that hepatic immunoreactivity of the pSer293 antibody is directly correlated with BCKD activity state (25). To examine the effect of an increased body load of leucine and KIC, we administrated leucine suspension or vehicle to mice using oral gavage, as elevated plasma leucine would be rapidly converted to KIC in extrahepatic tissues and subsequently accumulate in the liver. After 30 minutes of leucine treatment, significant induction of pSer293 dephosphorylation was observed in liver samples isolated from WT mice, but the already elevated pSer293 phosphorylation was not affected in *PP2Cm*$^{-/-}$ liver (Figure 4, B–E). Thus, PP2Cm is an essential phosphatase for the dephosphorylation of E1α in vivo, either at normal or elevated BCAA/BCKA concentrations, further supporting the idea that PP2Cm is indeed the indispensable endogenous BCKD phosphatase.

PP2Cm interacts with the BCKD complex through E2 and E1α subunits. To characterize the molecular mechanism underlying the specificity and function of PP2Cm as an E1α phosphatase, we first examined the interaction among PP2Cm and different subunits of the BCKD complex. Using an in vitro pull down assay, recombinant PP2Cm–glutathione-*S*-transferase (PP2Cm-GST) fusion protein showed direct interaction with recombinant His-tagged E2, whereas its binding with His-tagged E1α was much weaker and no direct interaction was detected with either the E1β or the E3 subunit under the same condition (Figure 5A). Although this result suggests that PP2Cm is recruited to its E1α substrate via direct binding to the E2 subunit, similar to what has been described for the BCKD kinase (26), the functional significance of its interaction with E1α and E1β subunits remains to be determined, as the E1 component of BCKD normally exists as a thiamine diphosphate-containing heterotetramer. The interaction between PP2Cm and BCKD was independent of PP2Cm phosphatase activity, since mutations of 3 residues required for PP2Cm catalytic activity (H129A, R236G, and D298A) (23) had no significant effect on PP2Cm interaction with E1α or E2 when overexpressed in COS7 cells (Figure 5B). In contrast, a PP2Cm mutant (PP2Cm-MD) lacking the mitochondrial targeting signal (23) had much diminished binding activity with the endogenous E2 or E1α (Figure 5B), sup-

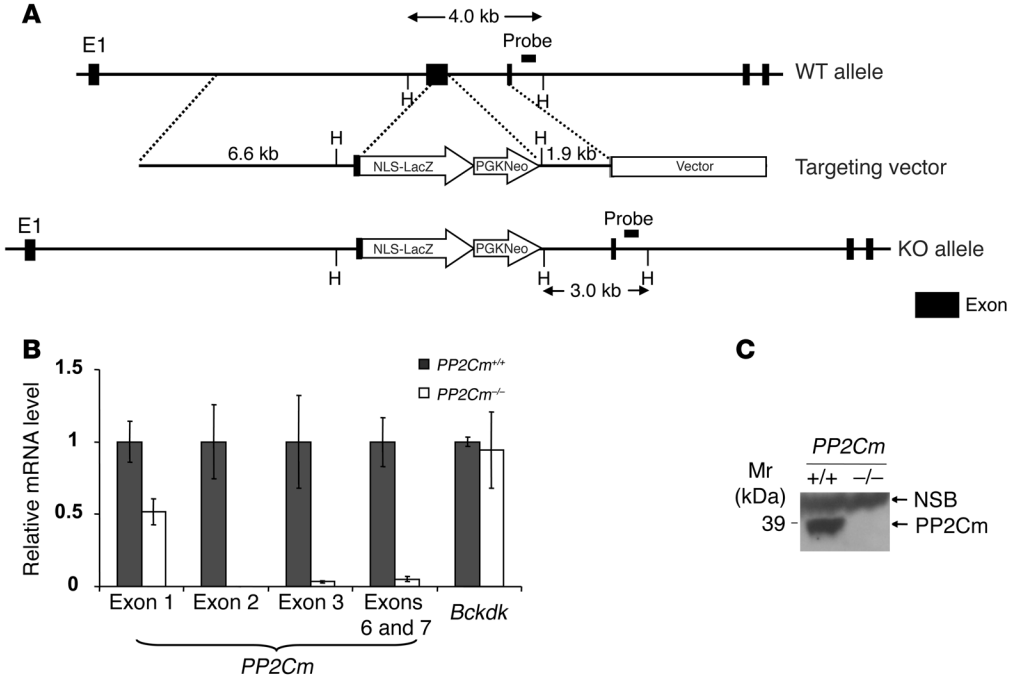

Figure 2
Generation of *PP2Cm*$^{-/-}$ mice. (**A**) Schematic illustration of gene-targeting strategy for the mouse *PP2Cm* gene. The NLS-LacZ (nuclear-localized lacZ) fragment was used to replace the coding sequence of *PP2Cm* in exon 2. (**B**) Real-time RT-PCR analysis of mRNA levels of BCKD kinase and *PP2Cm* in the heart, using primers against different PP2Cm exons as indicated. The relative mRNA levels were normalized against GAPDH and shown as relative levels to the signals from *PP2Cm*$^{+/+}$ exon 1. The results were generated from 3 independent experiments and are shown as mean ± SEM. (**C**) Immunoblot analysis of total heart lysate from *PP2Cm*$^{+/+}$ and *PP2Cm*$^{-/-}$ mice using anti-PP2Cm–specific polyclonal antibody. H, HindIII; NSB, nonspecific band.

porting the notion that full binding activity requires colocalization of PP2Cm and BCKD complex in mitochondria. We also sought to address whether Ser293 and/or Ser303 residues of E1α were required for E1α interaction with PP2Cm. As shown in Figure 5C, substitution of Ser293, but not Ser303, to Ala substantially abrogated E1α interaction with PP2Cm, implying that Ser293 was the critical residue for PP2Cm binding, consistent with it being the critical phosphorylation/dephosphorylation residue targeted by both BCKD kinase and PP2Cm.

Nutrient signal differentially affects BCKD interaction with PP2Cm and BCKD kinase. BCKD activity is potently activated by elevated BCKA concentration via E1α dephosphorylation, yet the underlying molecular mechanisms responsible for this remain unclear. In the PP2Cm-FLAG–expressing HEK293 cells, incubation with 5 mM BCKA for 3 days led to marked Ser293 dephosphorylation, while total protein levels of BCKD subunits (E1α, E1β, and E2) were not affected (Figure 5D). In BCKD immunocomplexes isolated with anti-E1α antibody, the BCKD kinase was dramatically depleted to a nondetectable level after 1-hour exposure to BCKA, while PP2Cm-FLAG was only modestly reduced at this time point. After 3-day BCKA treatment, BCKD kinase levels remained very low in the BCKD complex, and PP2Cm-FLAG protein levels also showed marked reduction (Figure 5E). This result is consistent with a previous study demonstrating that elevated BCKA levels can prevent the association of BCKD kinase with the BCKD complex (22). Consistent with this observation, concentrations of BCKD subunits were gradually reduced in the PP2Cm immunocomplex over time as demonstrated by immunoprecipitation with anti-FLAG antibody (Figure 5F). Therefore, α-ketoacid substrates induced an immediate dissociation of BCKD kinase from the BCKD complex; in contrast, the PP2Cm interaction with the BCKD complex was only affected after longer periods of exposure. The differential impact of the nutrient signal on PP2Cm versus BCKD kinase interaction with the enzyme complex provides a potential molecular basis for the rapid Ser293 dephosphorylation of E1α when plasma BCAA concentrations increase (Figure 5F).

PP2Cm deficiency impaired the catabolism of BCAA and BCKA in mice. Because the phosphorylation level of E1α at Ser293 inversely correlates with the plasma level of leucine (25), we asked whether the plasma level of BCAA was altered in *PP2Cm*$^{-/-}$ mice in which hepatic E1α was constitutively hyperphosphorylated. As shown in Figure 6A, plasma BCAA concentrations were indeed significantly higher in randomly fed *PP2Cm*$^{-/-}$ mice compared with WT controls of the same genetic background (*PP2Cm*$^{-/-}$, 1,122 ± 79 μM; $n = 9$ vs. WT, 691 ± 111 μM; $n = 8$; $P < 0.05$). In WT mice deprived of food for 6 hours, an i.p. injection of leucine increased the plasma BCAA level to approximately 950 μM in 30 minutes, which then recovered to near the basal level after 1 hour ($n = 4$; Figure 6B). However, the same leucine administration in *PP2Cm*$^{-/-}$ mice led to higher BCAA concentrations, approximately 1,500 μM at 30 minutes, which remained elevated over time compared with the WT controls, even after 4 hours (Figure 6, B and C). In response to a higher dose of leucine administrated orally to animals deprived of food overnight, *PP2Cm*$^{-/-}$ mice also had approximately 2-fold higher plasma BCAA levels than the WT mice (Figure 6D). The plasma levels of BCKA were higher, or trended to be higher, in vehi-

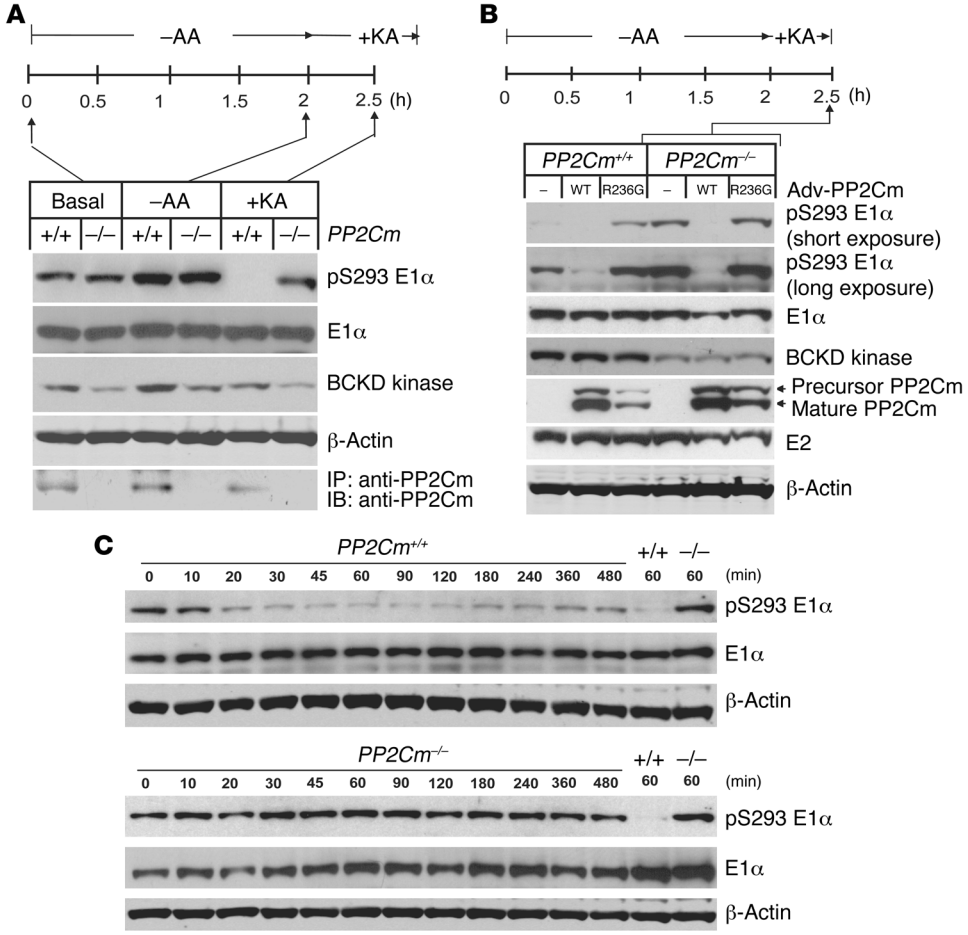

Figure 3

PP2Cm is the essential BCKD phosphatase in vitro. (**A**) *PP2Cm*$^{+/+}$ and *PP2Cm*$^{-/-}$ MEFs were first incubated in Krebs-Ringer-HEPES media at 37°C for 2 hours (basal conditions [Basal] and amino acid starvation [–AA]) and then treated with DMEM culture medium containing 5 mM each of the BCKA for an additional 30 minutes (treatment of BCKA [+KA]) as illustrated. Total cell lysates collected at different time points were subjected to immunoblotting analysis using anti–pSer293 E1α antibodies, BCKD kinase, and β-actin as indicated. PP2Cm protein was detected by immunoprecipitation and subsequent immunoblot using PP2Cm antibody as described (23). (**B**) *PP2Cm*$^{+/+}$ and *PP2Cm*$^{-/-}$ MEFs were infected with MOI 50 of Adv-PP2Cm (WT) or Adv–PP2Cm-R236G (R236G) for 48 hours. Cells were challenged by media containing 5 mM each of the BCKA for 30 minutes, and total cell lysates were analyzed by immunoblotting with the antibodies as indicated. (**C**) *PP2Cm*$^{+/+}$ or *PP2Cm*$^{-/-}$ MEFs were stimulated with media containing 5 mM each of the BCKA in culture medium for up to 8 hours. The pSer293 and total E1α were measured by immunoblotting as indicated. The last 2 lanes were loaded with additional *PP2Cm*$^{+/+}$ and *PP2Cm*$^{-/-}$ samples from the 60-minute time point as internal controls.

cle-treated *PP2Cm*$^{-/-}$ mice compared with WT mice (Figure 6, E–G). Thirty minutes after leucine administration, plasma BCKA concentrations were not changed significantly in WT animals (Figure 6, E–G), even though their plasma BCAA concentrations rose by an approximately 4-fold increase (leucine treated, 3,963 ± 461 μM vs. saline treated, 969 ± 235 μM; $P < 0.05$; Figure 6D) at the same time point, suggesting a robust clearance capacity for BCKA. In contrast, the plasma KIC concentration in *PP2Cm*$^{-/-}$ animals rose dramatically, by a more than 8-fold increase (leucine treated, 413.5 ± 43.4 μM vs. saline treated, 47.9 ± 8.2 μM; $P < 0.001$; Figure 6E). These data clearly indicate that loss of *PP2Cm* leads to elevated BCAA plasma concentration and impaired BCKA clearance, as would be expected for BCKD deficiency in MSUD patients.

Loss of PP2Cm increases reactive oxygen species. Elevated lipid peroxidation and impaired antioxidant defense have been implicated in human MSUD patients, indicative of increased level of oxidative stress (27–29). In addition, it has been shown that BCKA treatment triggers elevation of reactive oxygen species in cells and animals, presumably through cytotoxic inactivation of superoxide dismutase and glutathione peroxidase (30, 31). To investigate whether PP2Cm deficiency also resulted in induction of oxidative stress, we measured the level of reactive oxygen species in *PP2Cm*$^{-/-}$ and WT MEFs using dichlorodihydrofluorescein diacetate (DCF-DA) fluorescent dye. Reactive oxygen species levels were significantly ($P < 0.05$) higher in *PP2Cm*$^{-/-}$ MEFs compared with WT MEFs, either before or after incubation with BCKA (Figure 7A). Superoxide concentrations were also significantly ($P < 0.05$) higher in *PP2Cm*$^{-/-}$ compared with WT MEFs. Importantly, superoxide levels in both WT and *PP2Cm*$^{-/-}$ MEFs were significantly decreased by ectopically expressed WT PP2Cm (Figure 7B), clearly demonstrating that PP2Cm deficiency was the specific cause of the increased oxidative stress. More significantly, in all *PP2Cm*$^{-/-}$

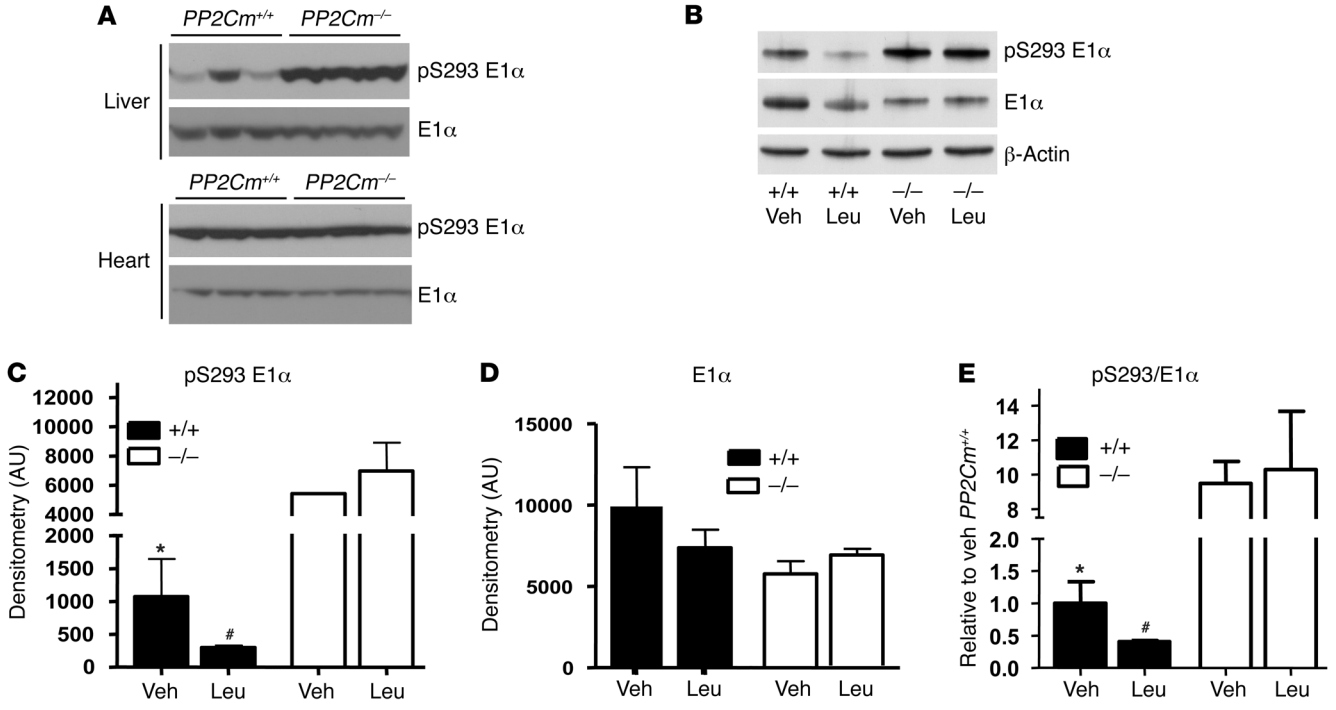

Figure 4

PP2Cm is the essential BCKD phosphatase in vivo. (**A**) Immunoblotting analysis of total tissue lysates from the liver (top panel) and heart (bottom panel) of *PP2Cm*$^{+/+}$ and *PP2Cm*$^{-/-}$ mice, for both total and pSer293 E1α as indicated. (**B**) Representative immunoblots of liver lysate for pSer293 E1α, total E1α, and β-actin from *PP2Cm*$^{+/+}$ and *PP2Cm*$^{-/-}$ mice 30 minutes after oral administration with either saline vehicle (Veh) or leucine (Leu) as described in Methods. (**C**–**E**) The relative levels of pSer293 E1α (**C**) and total E1α (**D**) and their ratio (**E**) from *PP2Cm*$^{+/+}$ and *PP2Cm*$^{-/-}$ livers were quantified. The quantification of the pSer293 to total E1α ratio was normalized against vehicle-treated WT mice. All bar graphs represent mean ± SEM. **P* < 0.01, saline-treated *PP2Cm*$^{-/-}$ versus *PP2Cm*$^{+/+}$mice; $^{\#}P$ < 0.01, leucine-treated versus saline-treated *PP2Cm*$^{+/+}$ mice.

tissues tested, including aorta, liver, and lung, there was a marked induction of superoxide level relative to the WT controls (Figure 7C and Supplemental Figure 4). Thus, PP2Cm deficiency led to oxidative stress both in vitro and in vivo.

Loss of PP2Cm sensitizes neonates to premature death when fed a high-protein diet. Classic type MSUD patients develop adverse symptoms soon after birth and have high postnatal mortality in the absence of proper dietary control. When *PP2Cm*$^{+/-}$ females were bred with *PP2Cm*$^{-/-}$ males and fed a high-protein diet during and after their pregnancies, the *PP2Cm*$^{-/-}$ offspring had a substantially higher incidence of premature death compared with *PP2Cm*$^{+/-}$ littermates (Figure 7D).

Discussion

We report here that a mitochondrial matrix protein, PP2Cm, is the endogenous phosphatase essential for the regulation and nutrient-induced activation of the rate-limiting step in BCAA metabolism catalyzed by the BCKD. This claim is based on several lines of evidence. First, PP2Cm specifically interacted with the BCKD complex via direct binding with its E2 subunit and, to a lesser degree, with its E1α subunit. Second, PP2Cm specifically and efficiently dephosphorylated Ser293 of the E1α subunit at pSer293, which is required for reactivation of BCKD. Third, loss of either PP2Cm expression or activity resulted in a loss of ability to dephosphorylate Ser293 E1α in response to BCKA stimulation in vivo. Finally, loss of PP2Cm expression in intact animals impaired BCAA catabolism, leading to elevated plasma BCAA and BCKA concentrations. When fed a high-protein diet, *PP2Cm*$^{-/-}$ mice developed characteristic features of human MSUD, induction of oxidative stress and neonatal lethality.

Discovery of the molecular identity of the BCKD phosphatase has multifaceted significance. The first aspect is historical. BCKD is a highly conserved, multisubunit enzyme complex mediating the rate-limiting and first committed step of oxidative decarboxylation of BCAA, whose activity is essential to normal cellular growth and function from single cell organisms to mammals. It has long been established that BCKD enzymatic activity is determined by the phosphorylation status of its E1α subunit. The BCKD kinase was purified and had its molecular identity determined almost 2 decades ago (20, 21, 32). However, the putative BCKD phosphatase thought to be responsible for its activation proved more elusive. In the 1980s, Reed's laboratory purified a novel Mn^{+2}/Mg^{+2}-independent phosphatase and posited that this enzyme was the BCKD phosphatase (18, 33). Unfortunately, subsequent attempts by others to purify the BCKD phosphatase were apparently unsuccessful, and its molecular identity remained unresolved. Recently, our laboratory identified PP2Cm as a mitochondrial phosphatase that appeared to be essential for development and regulation of the mitochondrial transition pore; however, its substrate was not known (23). Shortly thereafter, Joshi et al. (14) showed that PP2Cm could dephosphorylate BCKD in vitro. However, many protein phosphatases possess this activity in the test tube, including alkaline phosphatase and PP2A. Notably, the molecular weight of PP2Cm (~41 kDa) and the metal dependence of the PP2C family did not match the enzyme

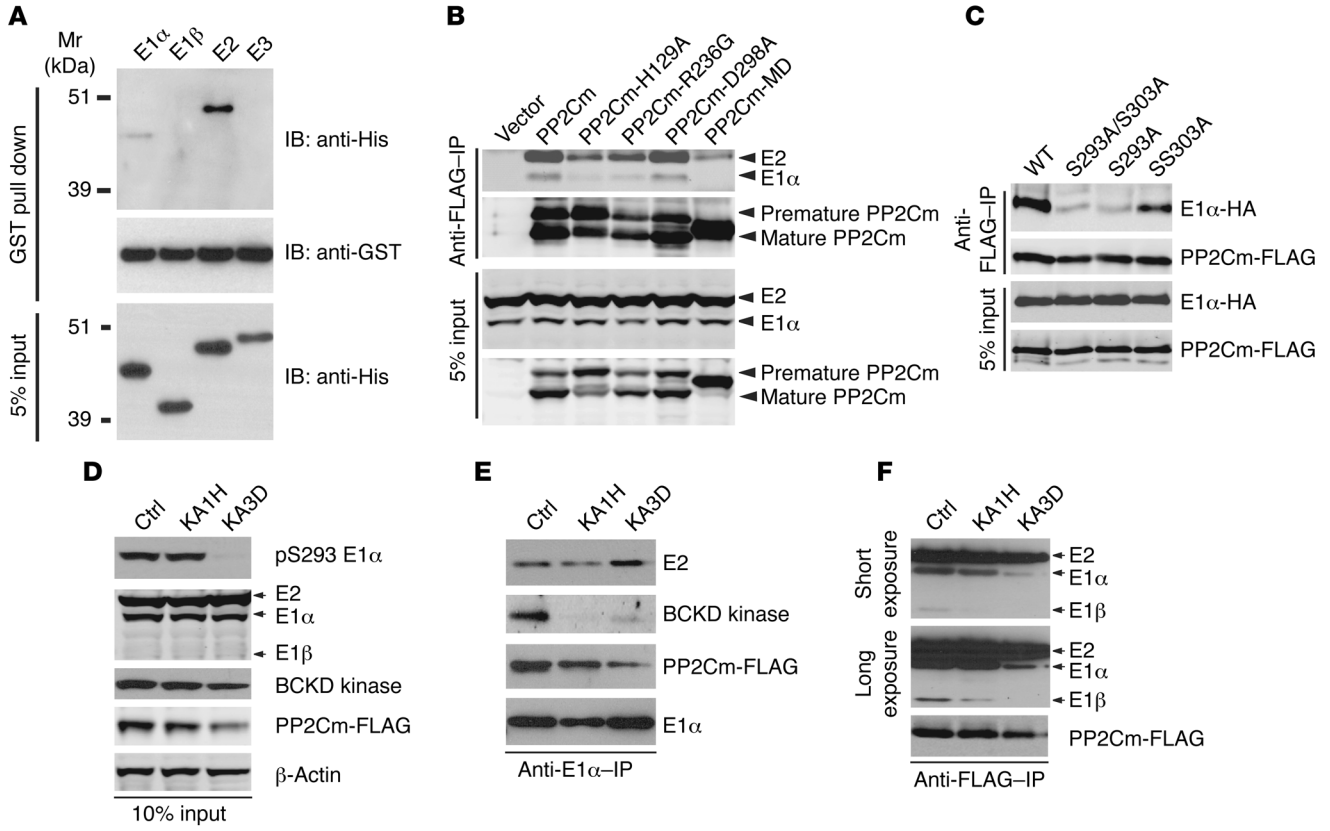

Figure 5

Specific association of PP2Cm with the BCKD complex. (**A**) Glutathione-S-transferase (GST) immunoprecipitation followed by anti-His or anti-GST immunoblotting, after incubation of GST-PP2Cm with His-tagged BCKD subunits as indicated. Five percent of the total input for the immunoprecipitation assay was also subjected to immunoblotting as shown. (**B**) COS7 cells were infected with adenoviruses expressing FLAG-tagged *PP2Cm* WT or mutants (H129A, R236G, D298A, and mitochondria-targeting defective [MD]) as indicated (MOI 50). Twenty-four hours later, total cell lysates were immunoprecipitated with M2 beads, followed by immunoblotting using anti-E1/E2 and anti-PP2Cm antibodies as indicated. The full-length PP2Cm (premature) and cleaved PP2Cm (mature) proteins were detected. (**C**) PP2Cm-FLAG was coexpressed with either HA-tagged WT E1α (E1α-HA) or mutants (Ser293A, Ser303A, and E1α-Ser293A/Ser303A) in HEK293T cells. Immunoblotting for E1α and PP2Cm in total cell lysates (input) or anti-FLAG immunoprecipitates are shown as indicated. (**D**–**F**) PP2Cm-FLAG–expressing 293T cells were treated with 5 mM BCKA for 1 hour (KA1H) or 3 days (KA3D). Total cell lysates were analyzed by immunoblot directly with the antibodies as labeled (**D**) or following immunoprecipitation with anti-E1α (**E**) or anti-FLAG (**F**) antibodies.

purified by Reed's laboratory (~33 kDa). Using an unbiased proteomic approach, starting with PP2Cm, rather than BCKD complex, we found BCKD components to be the main specific protein species associated with PP2Cm. The empirical evidence from both gain- and loss-of-function studies in intact cells and animals unequivocally establish PP2Cm as the endogenous BCKD phosphatase.

These findings provided new insights into the previously unexplored molecular mechanisms for nutrient-mediated regulation of BCAA catabolism. We have established here the molecular basis of PP2Cm interaction with the BCKD complex and identified Ser293 phosphorylation of E1α as a requirement for PP2Cm recruitment into the BCKD complex, most likely via E2 subunit interaction. Although we have evidence for a direct interaction between PP2Cm and the E1α subunit, but not the E1β subunit, their interaction in intact BCKD complex remains to be determined. The E1 component exists as $\alpha 2\beta 2$ tetramer, and the monomeric recombinant subunits might not have the same conformation for protein-protein interaction as those in vivo. We have further demonstrated that there exists a differential impact on the dissociation of the BCKD kinase versus PP2Cm upon substrate stimulation. These new insights provide a better understanding to the underlying regulatory mechanisms involved in BCAA metabolism under physiological conditions.

Last, the establishment of a *PP2Cm*$^{-/-}$ mouse model provides us an in vivo system to test the physiological importance and pathological implications of PP2Cm in BCKD regulation. As discussed earlier, inherited mutations of BCKD subunits cause MSUD in humans with a spectrum of severity. According to the variation in clinical consequences and genetic testing, human MSUD is categorized into 5 types: classic, intermediate, intermittent, thiamine responsive, and E3 deficient (8, 34). Our data clearly demonstrate that loss of *PP2Cm* leads to a metabolic and phenotypic abnormality characteristic of intermittent or intermediate types of human MSUD. Homanics et al. (35) have generated an MSUD model by genetic targeting of the E2 subunit of BCKD; these mice have severe postnatal developmental problems unless they are rescued by hepatic-specific expression of the human E2 subunit, thus representing a model of the "classic" types of MSUD. In contrast, the

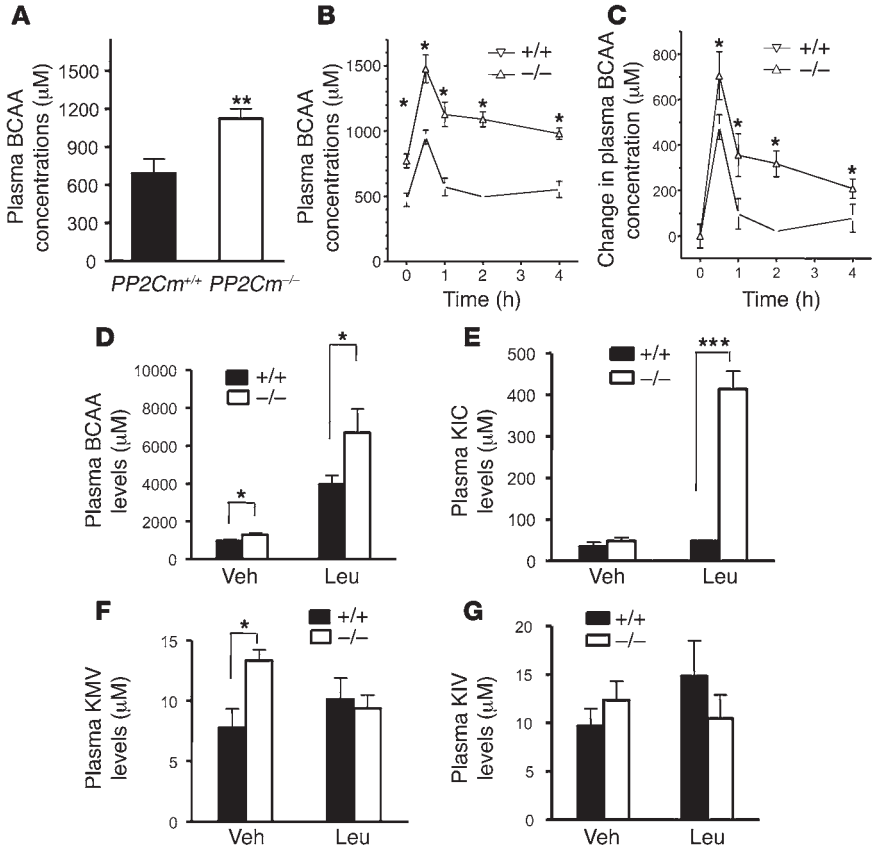

Figure 6
BCAA catabolic defects in *PP2Cm*-deficient mice. (**A**) Plasma concentrations of BCAA in randomly fed *PP2Cm*$^{+/+}$ (n = 8) and *PP2Cm*$^{-/-}$ (n = 9) mice. Results are presented as mean ± SEM. $^{**}P < 0.05$, Student's t test. (**B** and **C**) WT (n = 4) and *PP2Cm*$^{-/-}$ (n = 4) mice were fasted for 6 hours and then i.p. administered a 150-mM leucine solution. Blood samples were collected and BCAA were measured at different time points as indicated. The changes in total (**B**) and baseline-corrected (**C**) plasma levels of BCAA upon leucine challenge are presented as mean ± SEM. $^{*}P < 0.05$, Student's t test. (**D**–**G**) Plasma levels of BCAA (**D**), KIC (**E**), α-keto-β-methylvalerate (KMV) (**F**), and α-ketoisovalerate (KIV) (**G**) in WT (black bars) and *PP2Cm*$^{-/-}$ (white bars) animals 30 minutes after oral administration of 1.027 M leucine slurry (n = 5–6) or saline (n = 3) following overnight fast. Results are presented as mean ± SEM. $^{*}P < 0.05$, $^{***}P < 0.001$, Student's t test.

PP2Cm$^{-/-}$ mice, reported herein, thrive well under normal conditions, exhibiting no overt developmental issues. However, symptoms of MSUD in humans can be either initiated or abrogated through dietary manipulation. The fact that the *PP2Cm*$^{-/-}$ mice display this same behavior — that is, experimental changes in the nutritional conditions induce manifestation of MSUD phenotypes — provides a tremendous opportunity to examine the molecular mechanisms underlying the impact of diet on neural toxicity and mitochondrial dysfunction in vivo. Moreover, this model will facilitate the distinguishing of the diet-induced effects from the overt postnatal toxicity and developmental issues that appear in the E2 knockout mice. Together, these models now endow a more informed dissection of the myriad of clinical presentations of MSUD. Finally, at least 5 human SNPs have been identified in the PP2Cm coding sequence that can cause loss of function to the protein (Supplemental Figure 5); therefore, PP2Cm dysfunction is potentially a new etiology for certain types of MSUD in humans and may be a new therapeutic target for the disease. Furthermore, BCAA oxidation is elevated and dysregulated in a number of catabolic diseases and conditions, including acidosis, alcoholism, following burns, diabetes mellitus, or infection/sepsis, and during cancer cachexia. Identification of PP2Cm as the BCKD phosphatase will permit investigations into the role of this enzyme in dysregulated BCAA oxidation associated with these diseases.

Methods

Cell cultures, plasmids, and adenoviral vectors. HEK293T, COS7, and primary E12.5 MEFs were as described in Supplemental Methods. Pancreatic β cell lines INS-1 and INS-1/Flp-In T-REX were a gift from Gerhart U. Ryffel (Universitätsklinikum Essen, Essen, German). Plasmid and adenoviral vectors used in this paper were described in detail in Supplemental Methods.

Mass spectrometry. Proteins were digested with trypsin, as described by Shevchenko et al., and analyzed by LC/MS/MS on a Thermo LTQ Orbitrap mass spectrometer with an Eksigent NanoLC pump (36). The peptides were loaded onto a C18 reverse-phase column at a flow rate of 3 μl/min. Mobile phase A was 0.1% formic acid and 2% ACN in water; mobile phase B was 0.1% formic acid and 20% water in ACN. Peptides were eluted from the column at a flow rate of 220 nl/min, using a linear gradient from 5% B to 50% B over 90 minutes, then to 95% B over 5 minutes, and finally keeping constant 95% B for 5 minutes. Spectra were acquired in data-dependent mode with the Orbitrap used for mass spectrometry scans and LTQ for tandem mass spectrometry. Peptides were identified by searching the spectra against the rat International Protein Index (version 3.34; http://www.ebi.ac.uk/IPI/IPIhelp.html), using the SEQUEST algorithm integrated into the BioWorks software package. Each peptide met the following criteria: XCorr ≥2 (for +1 ions), ≥3 (for +2 ions), and ≥4 (for +3 ions) and DeltaCN >0.1. All proteins were identified on the basis of 2 or more peptides, and all spectra were manually interpreted.

Gene targeting. The murine *PP2Cm* gene was targeted in Sv129 ES cells. The first 440-nt PP2Cm encoding sequence in exon 2 was replaced by a nuclear LacZ expression cassette and a PGKNeo cassette. The 6.6-kb 5′-homology arm and 1.9-kb 3′-homology arm were amplified from a Sv129 BAC clone containing *PP2Cm* gene by PCR using PFU polymerase (Stratagene). The homologous recombination was confirmed by Southern blot by using external probes. Two individually isolated heterozygous ES clones were used to establish PP2Cm founder chimera. The resultant PP2Cm heterozygous mice were bred to generate PP2Cm homozygous mice.

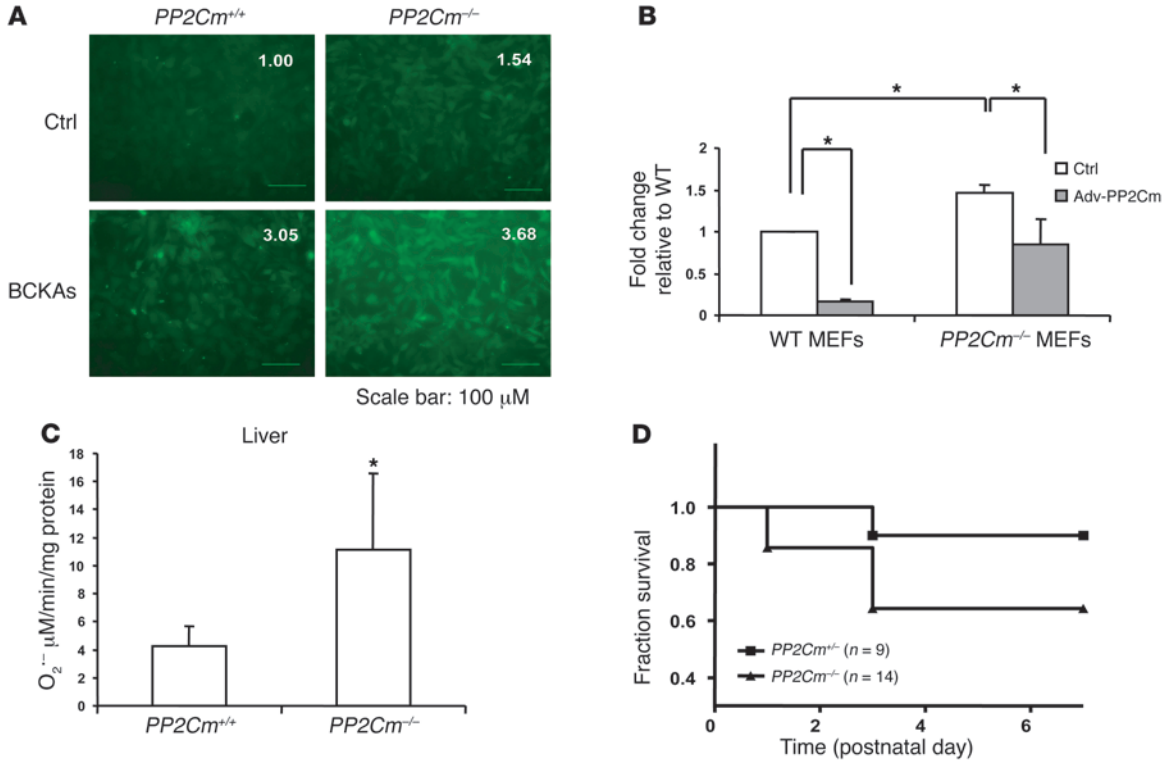

Figure 7
Oxidative stress in *PP2Cm*-deficient cells and tissues. (**A**) Representative dichlorodihydrofluorescein diacetate (DCF-DA) fluorescence images of *PP2Cm*$^{+/+}$ and *PP2Cm*$^{-/-}$ MEFs treated with or without 5 mM BCKA at 37°C for 30 minutes. Fluorescent signals were recorded digitally under the same setting, and the relative fluorescence intensity compared with the control is shown as labeled. Scale bars: 100 μm. (**B**) Electron spin resonance measurement of superoxide level in WT and *PP2Cm*$^{-/-}$ MEFs under basal conditions, infected with (gray bars) or without (white bars) Adv-PP2Cm (MOI = 100). Results are presented as mean ± SEM. **P* < 0.05, Student's *t* test. (**C**) Electron spin resonance measurement of superoxide production in liver from randomly fed animals. Results are presented as mean ± SEM. **P* < 0.05, Student's *t* test. (**D**) Survival curve of offspring from the breeding of male *PP2Cm*$^{-/-}$ mice and female *PP2Cm*$^{+/-}$ mice fed a high-protein diet.

Real-time RT-PCR analysis. Total RNA was extracted from cells or tissues using TRIzol Reagent (Invitrogen) according to manufacturer's instructions. Total RNA was reverse transcribed into the first-strand cDNA using the SuperScript First-Strand Synthesis Kit (Invitrogen). Then, cDNA transcripts were quantified by the iCycler iQ Real-Time PCR Detection System (Bio-Rad), using iQ SYBR Green Supermix (Bio-Rad). Each reaction was performed in duplicate, and values were averaged to calculate the relative expression level. Primer sequences are provided in Supplemental Methods.

Superoxide detection in cells and tissues. DCF-DA staining and electron spin resonance were used to measure the superoxide level in cultured cells and mouse tissues. Details of the experimental procedures are provided in Supplemental Methods.

BCKA challenge in MEFs and leucine challenge in mice. MEFs were washed twice with Krebs-Ringer-HEPES buffer and incubated in the same buffer for 2 hours, followed by the addition of fresh culture medium containing, a mixture of all of the BCKA at 5 mM for 30 minutes. Total cell lysates were collected at different time points and subjected to immunoblotting analysis. For leucine tolerance test in vivo, 6-hour food-deprived mice that were deprived of food for 6 hours were i.p. injected with 150 mM leucine solution at the dose of 15 μl/g body weight. Blood samples were collected at 0, 0.5, 1, 2, and 4 hours after leucine administration for plasma BCAA measurements. For Ser293 E1α phosphorylation and alterations in response to plasma BCKA, overnight (16-hour) fasted mice were orally gavaged with either a leucine slurry solution (1.027 M in saline) or saline vehicle in the amount of 15 μl/g body weight. Mice were sacrificed at 30 minutes after leucine administration, and blood and liver samples were collected.

BCAA and BCKA analysis. Total plasma BCAA concentrations were also measured by an enzymatic method using leucine dehydrogenase (Toyono Co.) (37). Individual BCKA were determined by HPLC as described by Loi et al. (38).

Animal handling and usage. The experiments with animals were reviewed and approved by the IACUCs of UCLA and Penn State College of Medicine.

Statistics. A 2-tailed Student's *t* test was performed to determine the significance of differences between control and PP2Cm knockout groups. A *P* value of less than 0.05 was considered significant.

Acknowledgments

The authors wish to thank Haiying Pu, Stephanie Goshorn, and Beth Gern for excellent technical assistance, as well as William J. Zinnanti and Kathleen Griffin for help with BCKA assays. This study was supported in part by NIH grants HL080111, HL70079, and HL62311 (to Y. Wang), HLP01-008111 (to P. Ping), HL087132 and RR 022371 (to T.M. Vondriska), DK053843 and DK062880 (to C.J. Lynch); the Laubisch Fund (UCLA); and American Heart Association (AHA) Western States Affiliate Predoctoral Fellowship Award (to G. Lu); AHA Postdoctoral Fellowship Award (to H. Sun); and AHA Established Investigator Award (to Y. Wang).

Received for publication November 25, 2008, and accepted in revised form February 25, 2009.

Address correspondence to: Yibin Wang, Division of Molecular Medicine, Departments of Anesthesiology, Physiology, and Medicine, Cardiovascular Research Laboratories, Molecular Biology Institute, UCLA David Geffen School of Medicine, Room BH 569, CHS650 Charles E. Young Drive, Los Angeles, California 90095, USA. Phone: (310) 206-5197; Fax: (310) 206-5907; E-mail: yibinwang@mednet.ucla.edu.

1. Harper, A.E., Miller, R.H., and Block, K.P. 1984. Branched-chain amino acid metabolism. *Annu. Rev. Nutr.* **4**:409–454.
2. Hutson, S.M., Sweatt, A.J., and Lanoue, K.F. 2005. Branched-chain [corrected] amino acid metabolism: implications for establishing safe intakes. *J. Nutr.* **135**:1557S–1564S.
3. Donato, J., Jr., Pedrosa, R.G., Cruzat, V.F., Pires, I.S., and Tirapegui, J. 2006. Effects of leucine supplementation on the body composition and protein status of rats submitted to food restriction. *Nutrition.* **22**:520–527.
4. Layman, D.K., and Walker, D.A. 2006. Potential importance of leucine in treatment of obesity and the metabolic syndrome. *J. Nutr.* **136**:319S–323S.
5. Zhang, Y., Guo, K., LeBlanc, R.E., Loh, D., Schwartz, G.J., and Yu, Y.H. 2007. Increasing dietary leucine intake reduces diet-induced obesity and improves glucose and cholesterol metabolism in mice via multimechanisms. *Diabetes.* **56**:1647–1654.
6. Joshi, M.A., et al. 2006. Impaired growth and neurological abnormalities in branched-chain alpha-keto acid dehydrogenase kinase-deficient mice. *Biochem. J.* **400**:153–162.
7. Dancis, J., Levitz, M., Miller, S., and Westall, R.G. 1959. Maple syrup urine disease. *Br. Med. J.* **1**:91–93.
8. Dancis, J., Levitz, M., and Westall, R.G. 1960. Maple syrup urine disease: branched-chain keto-aciduria. *Pediatrics.* **25**:72–79.
9. Chuang, J.L., et al. 1995. Molecular and biochemical basis of intermediate maple syrup urine disease. Occurrence of homozygous G245R and F364C mutations at the E1 alpha locus of Hispanic-Mexican patients. *J. Clin. Invest.* **95**:954–963.
10. Hall, T.R., Wallin, R., Reinhart, G.D., and Hutson, S.M. 1993. Branched chain aminotransferase isoenzymes. Purification and characterization of the rat brain isoenzyme. *J. Biol. Chem.* **268**:3092–3098.
11. Hutson, S.M., Wallin, R., and Hall, T.R. 1992. Identification of mitochondrial branched chain aminotransferase and its isoforms in rat tissues. *J. Biol. Chem.* **267**:15681–15686.
12. Sweatt, A.J., et al. 2004. Branched-chain amino acid catabolism: unique segregation of pathway enzymes in organ systems and peripheral nerves. *Am. J. Physiol. Endocrinol. Metab.* **286**:E64–E76.
13. Chuang, D.T., Chuang, J.L., and Wynn, R.M. 2006. Lessons from genetic disorders of branched-chain amino acid metabolism. *J. Nutr.* **136**:243S–249S.
14. Joshi, M., Jeoung, N.H., Popov, K.M., and Harris, R.A. 2007. Identification of a novel PP2C-type mitochondrial phosphatase. *Biochem. Biophys. Res. Commun.* **356**:38–44.
15. Pettit, F.H., Yeaman, S.J., and Reed, L.J. 1978. Purification and characterization of branched chain alpha-keto acid dehydrogenase complex of bovine kidney. *Proc. Natl. Acad. Sci. U. S. A.* **75**:4881–4885.
16. Machius, M., et al. 2006. A versatile conformational switch regulates reactivity in human branched-chain alpha-ketoacid dehydrogenase. *Structure.* **14**:287–298.
17. Yeaman, S.J. 1989. The 2-oxo acid dehydrogenase complexes: recent advances. *Biochem. J.* **257**:625–632.
18. Damuni, Z., Merryfield, M.L., Humphreys, J.S., and Reed, L.J. 1984. Purification and properties of branched-chain alpha-keto acid dehydrogenase phosphatase from bovine kidney. *Proc. Natl. Acad. Sci. U. S. A.* **81**:4335–4338.
19. Harris, R.A., et al. 1997. Studies on the regulation of the mitochondrial alpha-ketoacid dehydrogenase complexes and their kinases. *Adv. Enzyme Regul.* **37**:271–293.
20. Shimomura, Y., Nanaumi, N., Suzuki, M., Popov, K.M., and Harris, R.A. 1990. Purification and partial characterization of branched-chain alpha-ketoacid dehydrogenase kinase from rat liver and rat heart. *Arch. Biochem. Biophys.* **283**:293–299.
21. Harris, R.A., et al. 1995. A new family of protein kinases--the mitochondrial protein kinases. *Adv. Enzyme Regul.* **35**:147–162.
22. Murakami, T., Matsuo, M., Shimizu, A., and Shimomura, Y. 2005. Dissociation of branched-chain alpha-keto acid dehydrogenase kinase (BDK) from branched-chain alpha-keto acid dehydrogenase complex (BCKDC) by BDK inhibitors. *J. Nutr. Sci. Vitaminol. (Tokyo).* **51**:48–50.
23. Lu, G., et al. 2007. A novel mitochondrial matrix serine/threonine protein phosphatase regulates the mitochondria permeability transition pore and is essential for cellular survival and development. *Genes Dev.* **21**:784–796.
24. Suryawan, A., et al. 1998. A molecular model of human branched-chain amino acid metabolism. *Am. J. Clin. Nutr.* **68**:72–81.
25. Lynch, C.J., et al. 2003. Potential role of leucine metabolism in the leucine-signaling pathway involving mTOR. *Am. J. Physiol. Endocrinol. Metab.* **285**:E854–E863.
26. Obayashi, M., Sato, Y., Harris, R.A., and Shimomura, Y. 2001. Regulation of the activity of branched-chain 2-oxo acid dehydrogenase (BCODH) complex by binding BCODH kinase. *FEBS Lett.* **491**:50–54.
27. Barschak, A.G., et al. 2008. Maple syrup urine disease in treated patients: biochemical and oxidative stress profiles. *Clin. Biochem.* **41**:317–324.
28. Barschak, A.G., et al. 2008. Oxidative stress in plasma from maple syrup urine disease patients during treatment. *Metab. Brain Dis.* **23**:71–80.
29. Barschak, A.G., et al. 2006. Evidence that oxidative stress is increased in plasma from patients with maple syrup urine disease. *Metab. Brain Dis.* **21**:279–286.
30. Funchal, C., et al. 2004. Evidence that the branched-chain alpha-keto acids accumulating in maple syrup urine disease induce morphological alterations and death in cultured astrocytes from rat cerebral cortex. *Glia.* **48**:230–240.
31. Funchal, C., et al. 2006. Morphological alterations and induction of oxidative stress in glial cells caused by the branched-chain alpha-keto acids accumulating in maple syrup urine disease. *Neurochem. Int.* **49**:640–650.
32. Davie, J.R., et al. 1995. Expression and characterization of branched-chain alpha-ketoacid dehydrogenase kinase from the rat. Is it a histidine-protein kinase? *J. Biol. Chem.* **270**:19861–19867.
33. Damuni, Z., and Reed, L.J. 1988. Branched-chain alpha-keto acid dehydrogenase phosphatase and its inhibitor protein from bovine kidney. *Methods Enzymol.* **166**:321–329.
34. Simon, E., Flaschker, N., Schadewaldt, P., Langenbeck, U., and Wendel, U. 2006. Variant maple syrup urine disease (MSUD)--the entire spectrum. *J. Inherit. Metab. Dis.* **29**:716–724.
35. Homanics, G.E., Skvorak, K., Ferguson, C., Watkins, S., and Paul, H.S. 2006. Production and characterization of murine models of classic and intermediate maple syrup urine disease. *BMC Med. Genet.* **7**:33.
36. Shevchenko, A., Wilm, M., Vorm, O., and Mann, M. 1996. Mass spectrometric sequencing of proteins silver-stained polyacrylamide gels. *Anal Chem.* **68**:850–858.
37. Beckett, P.R. 2000. Spectrophotometric assay for measuring branched-chain amino acids. *Methods Enzymol.* **324**:40–47.
38. Loi, C., Nakib, S., Neveux, N., Arnaud-Battandier, F., and Cynober, L. 2005. Ornithine alpha-ketoglutarate metabolism in the healthy rat in the postabsorptive state. *Metabolism.* **54**:1108–1114.